ANALYSIS OF TEMPERATURE VARIATIONS IN FIXED-BED COLUMNS USING NON-ISOTHERMAL AND NON-EQUILIBRIUM TRANSPORT MODEL

Shireen ZAFAR[a], Sadia PERVEEN[b*], Asad Tufail CHEEMA[a], and Shamsul QAMAR[a,c]

[a] Department of Mathematics, COMSATS University, Islamabad, Pakistan
[b] Department of Mathematics, AIR University, Islamabad, Pakistan
[c] Max Planck Institute for Dynamics of Complex Technical Systems Magdeburg, Magdeburg, Germany

Original scientific paper
https://doi.org/10.2298/TSCI200227192Z

A non-isothermal and non-equilibrium two-component lumped kinetic model of fixed-bed column liquid chromatography is formulated with the linearized isotherm and solved analytically to study the influence of temperature variations on the process. The model equations constitute a system of convection-diffusion PDE for mass and energy balances in the bulk phase coupled with differential equations for mass and energy balances in the stationary phase. The analytical solutions are derived for Dirichlet boundary conditions by implementing the Laplace transformation, Tschirnhaus-Vieta approach, the linear decomposition technique and an elementary solution technique of ODE. An efficient and accurate numerical Laplace inversion technique is applied to bring back the solution in the actual time domain. In order to validate the derived analytical solutions for concentration and temperature fronts, the high resolution upwind finite volume scheme is applied to approximate the model equations numerically. Various case studies are carried out assuming realistic model parameters. The results obtained will be beneficial for interpreting mass and energy profiles in non-equilibrium and non-isothermal liquid chromatographic columns and provide deeper insight into the sensitivity of the separation process without performing costly and time-consuming laboratory experiments.

Key words: *non-reactive chromatography, non-isothermal operation, thermal effects, lumped kinetic model, analytical solutions, finite volume scheme*

Introduction

Fixed-bed column chromatography is a very impressive technique to separate particles or molecules of a mixture by portioning characteristics of particles to keep in a stationary phase or in a mobile phase. It is a useful technique for the continuous separation of bulk multi-component mixtures and can be implemented for the separation of substances that are not feasibly separable by conventional processes, namely distillation or extraction. The technique is highly suitable for complicated separation tasks in which high purity of the product is of prime concern [1, 2]. A successful application of liquid chromatography technique to a particular problem demands suitable operation conditions. These conditions are influenced by types of column packing and mobile phase used, mobile-phase flow rate, the ratio of length and

* Corresponding author, e-mail: sadia.ahsan@mail.au.edu.pk

diameter of the column, column temperature, size of the sample, and so on. The selection of appropriate operating conditions needs a basic understanding of the assorted factors that manage liquid chromatography separation. The high performance liquid chromatography (HPLC) is normally carried out under isothermal condition by assuming the effect of adsorption heat as negligible. In recent years, the use of temperature as a separation parameter in the chromatographic separation process (elevated or unconventional) has gained attention as an additional valuable parameter for improving the HPLC analysis conditions [3-5]. The advantages of high temperature liquid chromatography (HTLC) technique include, reduction in retention time, improvement in efficiency of the column, better selectivity, reduced analysis time, lowered back pressure, reduction in organic concentration of mobile phase mixture and the use of temperature programming in liquid chromatography. Understanding the solute behavior at high temperature is fundamental to develop methods of HTLC analysis. Various authors have contributed to demonstrate the influence of high temperature on many practical applications, such as taking hot water as mobile phase in the chromatographic column are discussed in [6, 7]. The effect of temperature on the efficiency of column systems in adsorptive liquid chromatography are studied in [8]. A study to check the effect of temperature during a chromatographic phenomenon is made in [9]. Recently, the effect of forced temperature gradients introduced through heat exchange in liquid chromatography are theoretically studied in [10]. Several other contributions are also worthy to be considered [11-18]. To examine chromatographic separation at analytical and preparative levels, different models are accessible. A few of them, which are frequently considered, are the general rate model (GRM), the lumped kinetic model (LKM), and the equilibrium dispersive model (EDM). The general principle of the GRM is consideration of two fractions of the mobile phase. One fraction percolates through the column carrying the sample elements and the other one is the stagnant fraction inside the porous particles. The EDM assumes that each contribution of the non-equilibrium state can be lumped into a certain axial dispersion term. It simulate that the apparent dispersion coefficients of the solutes stay constant, independent of the concentration of sample elements. The LKM is composed of convection-diffusion PDE, coupled with algebraic and differential equations. The equations of mass balances are being coupled with kinetic equations which refer to the variation rate of concentrations in every segment of stationary phase to its concentrations in both phases, and to the equilibrium concentration inside the stationary phase. Each of these models consider different complexity levels to simulate the process.

In this research work, the non-equilibrium and non-isothermal two-component LKM is analytically and numerically analyzed. It extends and generalizes our recent work on the analysis of a single-solute model of non-isothermal liquid chromatography [19]. The considered non-equilibrium LKM is formed by convectiondiffusion PDE for mass and energy in the mobile phase coupled with differential equations for mass and energy in the stationary phase along with equilibrium equations for isotherms. Analytical solutions of the considered model are derived by assuming linearized equilibrium functions and Dirichlet boundary conditions. The Laplace transformation, Tschirnhaus-Vieta approach [20], the decoupling technique of linear transformation and an elementary solution technique of ODE are utilized to evaluate the analytical expressions for concentration and energy profiles in the Laplace domain [21, 22]. Moreover, the Laplace inversion is performed numerically to obtain the actual time domain solutions. A high resolution finite volume scheme (HR-FVS) is extended and applied to approximate the model equations numerically for non-linear isotherm [22]. Several case studies are considered to examine the influences of axial-dispersion, adsorption enthalpy, injected temperature, as well as mass and heat transfer rate coefficients on the elution profiles.

The non-equilibrium and non-isothermal chromatographic model

In this section, a two-component non-equilibrium and non-isothermal model of column liquid chromatography is formulated to study temperature effect on sample retention time, band broadening and separation process. The LKM of column chromatography assumes infinitely fast adsorption-desorption kinetics but the kinetic of mass transfer is slow. The model lumps the contributions of internal and external mass transport resistances within a single mass transfer coefficient and, thus, contains two essential kinetic parameters, the mass transfer coefficient and the axial dispersion which includes the band broadening effects caused by the packing quality. Moreover, the mobile phase concentration is assumed to be the same inside the pores of particles and in the bulk. The 1-D mass balance equations describing the transport of two-component solute through a chromatographic column along with an inert carrier are expressed:

$$\frac{\partial c_j}{\partial t} + u\frac{\partial c_j}{\partial z} = D_L\frac{\partial^2 c_j}{\partial z^2} - F\frac{\partial q_j}{\partial t},\ \ j = 1,2 \tag{1}$$

where $c_j(t, z)$ is the solute concentration of the j^{th} component in the mobile phase, $q_j(t, z)$ – the solute concentration in the stationary phase, u – the interstitial (fluid) phase velocity which is assumed to be constant, D_L – the axial dispersion coefficient which is assumed to be the same for both components, $F = (1 - \epsilon)/\epsilon$ – the phase ratio, $\epsilon \in (0,1)$ – the total porosity of column packing, z – the axial co-ordinate, and t – the time co-ordinate, respectively. In addition, the corresponding energy balance equation is expressed:

$$\frac{\partial T}{\partial t} + u\frac{\partial T}{\partial z} = \frac{\lambda_L}{C_{\text{f}}}\frac{\partial^2 T}{\partial z^2} + \sum_{j=1}^{2} F\frac{-\Delta H_{A,j}}{C_{\text{f}}}\frac{\partial q_j}{\partial t} - F\frac{C_{\text{e}}}{C_{\text{f}}}\frac{\partial T_S}{\partial t} \tag{2}$$

where T is the temperature of the mobile phase, λ_L – the effective axial heat conductivity coefficient, $\Delta H_{A,j}$ – the enthalpy of adsorption of j^{th} component, T_S – the temperature of stationary phase, $C_{\text{f}} = \rho^L c_P^L$ and $C_{\text{e}} = \rho^S c_P^S$. Here, ρ^S and ρ^L are the density per unit volume in the stationary phase and in the mobile phase, respectively, c_P^S and c_P^L – the corresponding heat capacities in the stationary and mobile phases. It is assumed that temperature does not influence viscosity, density, heat capacity, axial dispersion coefficients, as well as the axial heat conductivity coefficients. In this study, the considered densities ρ^L and ρ^S, and heat capacities c_P^L and c_P^S are taken independent of temperature. Further, the flow rate is assumed to be independent of axial dispersion and axial heat conductivity coefficients [23]. The LKM is a linear film driving force model that uses the first order kinetic equation to incorporate the non-equilibrium effects. Thus, the corresponding mass and heat balance equations for the mass and heat transfer kinetics in the stationary phase are expressed [23]:

$$\frac{\partial q_j}{\partial t} = k_j\left(q_j^* - q_j\right),\ \ j = 1,2 \tag{3}$$

$$\frac{\partial T_S}{\partial t} = \sum_{k=1}^{2}\frac{-\Delta H_{A,k}}{C_{\text{e}}}\frac{\partial q_k}{\partial t} + \frac{3h_p}{R_p C_{\text{e}}}\left(T - T_S\right) \tag{4}$$

where k_j is the j^{th} component rate coefficient of mass transfer, h_p – the heat transfer coefficient between the adsorbent stationary phase and the mobile phase, q_j^* – the j^{th} component equilibrium concentration of solute in the stationary phase, and R_p – the radius of spherical particles of adsorbent [24]. The considered non-isothermal two-component LKM given in eqs. (1)-(4), which is taking into account mass and heat transfer kinetics, is more accurate than the two-component non-isothermal EDM of our previous article [25]. For sufficiently large

mass and heat transfer coefficients, *i.e.* for $k_j \to \infty$ and $h_p \to \infty$, the solution of LKM converges to that of EDM. The equilibrium adsorption isotherm quantify the influence of temperature on the amount of solute adsorbed on the surface of solid. Using the enthalpy of adsorption, the van't Hoff type phase equilibrium relation can be expressed:

$$q_j^*(c_j, T_s) = a_j^{\text{ref}} c_j \exp\left[\frac{-\Delta H_{A,j}}{\text{R}_\text{g}}\left(\frac{1}{T_s} - \frac{1}{T_{\text{ref}}}\right)\right], \quad j = 1,2 \tag{5}$$

where a_j^{ref} is the j^{th} component reference Henry's constant, R_g – the general gas constant, and T^{ref} – the reference temperature. In order to facilitate our analysis, let us introduce the following transformation for temperature in the liquid and solid phases:

$$c_3 = T - T^{\text{ref}}, \quad q_3 = T_S - T^{\text{ref}} \tag{6}$$

Moreover, the following dimensionless variables are introduced in order to reduce the number of variables involved in the model equations and to simplify the notations:

$$x = \frac{z}{L}, \quad \tau = \frac{ut}{L}, \quad \text{Pe}_c = \frac{Lu}{D_L}, \quad \text{Pe}_h = \frac{LuC_\text{f}}{\lambda_L}, \quad H_L = \frac{3Lh_p}{uR_pC_\text{f}}, \quad H_S = \frac{3Lh_p}{uR_pC_\text{e}} \tag{7}$$

were L is the column length, while Pe_c and Pe_h are the Peclet numbers for concentration and temperature, respectively. On using eqs. (6) and (7) in eqs. (1) and (2), we obtain:

$$\frac{\partial c_m}{\partial \tau} + \frac{\partial c_m}{\partial x} = \frac{1}{\text{Pe}_m}\frac{\partial^2 c_m}{\partial x^2} - F\left\{\frac{\partial q_m}{\partial \tau} + H_L\left(c_3 - q_3\right)\delta_{3m}\right\}, \text{ where } \text{Pe}_m = \begin{cases} \text{Pe}_c, & \text{if } m = 1,2 \\ \text{Pe}_h, & \text{if } m = 3 \end{cases} \tag{8}$$

where δ_{lm} for $l = 3$ and $m = 1, 2, 3$ are the Kronecker delta function. Utilizing Taylor's expansion up to first order along with the assumption of small changes in concentration and temperature, the equilibrium relations between the mobile and solid phases can be easily linearized, *c.f.* eq. (5). Hence, for $j = 1, 2$, they are given in linearized form:

$$q_j^*\left(c_1, c_2, T\right) \approx q_j^*\Big|_{\left(c_1^{\text{ref}}, c_2^{\text{ref}}, T^{\text{ref}}\right)} + \sum_{j=1}^{2}\left(c_j - c^{\text{ref}}\right)\frac{\partial q_j^*}{\partial c_j}\Big|_{\left(c_1^{\text{ref}}, c_2^{\text{ref}}, T^{\text{ref}}\right)} + \left(T_\text{s} - T^{\text{ref}}\right)\frac{\partial q_j^*}{\partial T}\Big|_{\left(c_1^{\text{ref}}, c_2^{\text{ref}}, T^{\text{ref}}\right)} \tag{9}$$

After some manipulations and using eqs. (5) and (6), eq. (9) gives the linear system of equations:

$$q_j^*\left(c_1, c_2, q_3\right) = A_j c_j + B_j q_3, \quad j = 1,2 \text{ where } A_j = a_j^{\text{ref}}, \quad B_j = \frac{\Delta H_{A,j} a_j^{\text{ref}} c_j^{\text{ref}}}{\text{R}_\text{g} T^{\text{ref}^2}} \tag{10}$$

The initial conditions for an initially equilibrated column are defined:

$$c_m\left(x, 0\right) = c_{m,\text{init}}, \quad m = 1,2,3, \quad q_j\left(z, 0\right) = q_{j,\text{init}}^* \tag{11}$$

where $c_{3,\text{init}} = T_{\text{init}} - T^{\text{ref}}$. Here, $c_{j,\text{init}}$ ($j = 1, 2$) are the initial concentrations of mixture components and T_{init} – the initial temperature within a column. However, for an initially regenerated (cleaned) column the initial concentrations are zero, *i.e.* $c_{j,\text{init}} = 0$ ($j = 1, 2$). In addition, it is assumed that column is at reference temperature initially. The following boundary conditions are considered at both ends of the column:

$$c_m\left(x = 0, \tau\right) = \begin{cases} c_{m,\text{inj}}, & \text{if } 0 \le \tau \le \tau_{\text{inj}} \\ 0, & \tau > \tau_{\text{inj}} \end{cases}, \quad \frac{\partial c_m}{\partial x}\left(\infty, \tau\right) = 0, \quad m = 1,2,3 \tag{12}$$

where $c_{m,\text{inj}} = T_{m,\text{inj}} - T^{\text{ref}}$ and $\tau_{\text{inj}} = ut_{\text{inj}}/L$. Here, τ_{inj} stands for dimensionless injection time, $c_{j,\text{inj}}$ ($j = 1,2$) reveal the components of concentration in the injected pulse, and $T_{m,\text{inj}}$ represents the injected sample temperature. Primarily, in the practical application of liquid chromatog-

raphy, small values of the axial dispersion and heat conductivity coefficients are taken into account. Therefore, the considered Dirichlet BC are well applicable.

Derivation of analytical solution

The Laplace transformation can be applied to solve analytically the suggested linearized non-equilibrium and non-isothermal LKM along its associated initial, *c.f.* eq. (11), and boundary conditions, *c.f.* eq. (12). The Laplace transformation is defined:

$$\overline{c}_m\left(x,s\right)=\int_0^\infty \mathrm{e}^{-s\tau}c_m\left(x,\tau\right)\mathrm{d}\tau,\ \ m=1,2,3 \tag{13}$$

Substituting eq. (10) in eq. (3), then applying the Laplace transformation given by eq. (13) on the resulting equation yield:

$$\overline{q}_i=\frac{K_i}{s+K_i}\left(A_i\overline{c}_i+B_i\overline{q}_3\right)+\frac{1}{s+K_i}A_{ic_i,\mathrm{init}},\ \text{for}\ \ i=1,2 \tag{14}$$

$$\overline{q}_3=\frac{-\sum_{j=1}^{2}\left[s+\sum_{n=1}^{2}K_n\left(1-\delta_{jn}\right)\Delta H_{A,j}K_jA_j\right]}{\alpha}\left(s\overline{c}_j+c_{j,\mathrm{init}}\right)+\frac{H_SC_\mathrm{e}\left(s+K_1\right)\left(s+K_2\right)}{\alpha}\overline{c}_3 \tag{15}$$

where

$$\alpha=C_\mathrm{e}\left(s+H_S\right)\left(s+K_1\right)\left(s+K_2\right)+\sum_{j=1}^{2}\left[s+\sum_{n=1}^{2}K_n\left(1-\delta_{jn}\right)s\Delta H_{A,j}B_jK_j\right] \tag{16}$$

After applying the Laplace transformation on eq. (8) and plugging the values of $q_j(s)$ from eqs. (14) and (15), the resulting equation has the form:

$$\frac{1}{\mathrm{Pe}_m}\frac{\partial^2\overline{c}_m}{\partial x^2}-\frac{\partial\overline{c}_m}{\partial x}=\sum_{n=1}^{3}\beta_{mn}\left(s\overline{c}_n-c_{n,\mathrm{init}}\right),\ \ m=1,2,3 \tag{17}$$

where the new parameter introduced in eq. (17) can be expressed in tensor form:

$$\beta_{ii}=\left\{1+\sum_{l=1}^{2}\frac{FK_iA_i\delta_{il}}{s+K_i}-\frac{Fs\Delta H_{A,i}k_i^2A_iB_i\left[s+\sum_{j=1}^{2}k_j\left(1-\delta_{ij}\right)\right]}{\left(s+k_i\right)\alpha}\right\},\ \ i=1,2 \tag{18}$$

$$\beta_{33}=\frac{1}{s}\left[\left(s+FH_L\right)-\frac{FH_LH_sC_\mathrm{e}\left(s+k_1\right)\left(s+k_2\right)}{\alpha}\right],\ \ \beta_{ij}=\left[-\frac{Fs\Delta H_{A,j}K_iK_jA_jB_i}{\alpha}\right],\ \ i\neq j \tag{19}$$

$$\beta_{3j}=\left\{\frac{FH_L\Delta H_{A,j}K_jA_j\left[s+\sum_{l=1}^{2}k_l\left(1-\delta_{jl}\right)\right]}{\alpha}\right\},\quad \beta_{i3}=\left\{\frac{FH_sC_\mathrm{e}B_ik_i\left[s+\sum_{l=1}^{2}k_l\left(1-\delta_{il}\right)\right]}{\alpha}\right\},\ \ i,j=1,2 \tag{20}$$

Equation (17) represents a system of coupled equations. Hence, for analytical solution of these equations, first we have to decouple this system by applying the well-known eigen-decomposition approach. The matrix of coefficient, Q, on right hand side of eq. (17) in more simplified form can be written:

$$Q = \begin{pmatrix} \beta_{11} & \beta_{12} & \beta_{13} \\ \beta_{21} & \beta_{22} & \beta_{23} \\ \beta_{31} & \beta_{32} & \beta_{33} \end{pmatrix} \tag{21}$$

The aforementioned matrix will be diagonalizable, if it has three real and distinct eigenvalues. The characteristic equation for the coefficient matrix, Q, led us to cubic characteristic equation:

$$ax^3 + bx^2 + cx + d = 0 \tag{22}$$

where

$$a = 1,\ b = -\sum_{I=1}^{3} \beta_{ii},\ c = \sum_{i=1}^{3}\sum_{\substack{j=1 \\ j\neq i}}^{3} \left(\beta_{ii}\beta_{jj} - \beta_{ij}\beta_{ji}\right),\ d = -\det Q \tag{23}$$

Let us define:

$$A_1 = 2\sqrt{\frac{-p_1}{3}},\ w = \arccos\left(\frac{3p_2}{A_1 p_1}\right),\ A_2 = \frac{-b}{3a},\ p_1 = \frac{3ac - b^2}{3a^2},\ p_2 = \frac{2b^3 - 9abc + 27a^2 d}{27a^3} \tag{24}$$

The eigenvalues will be obtained as roots of the aforementioned characteristics eq. (22) by using the Tschirnhaus-Vieta approach and are given:

$$\lambda_m = A_1 \cos\left[\frac{u + (m-1)2\pi}{3}\right] + A_2,\ m = 1,2,3 \tag{25}$$

The corresponding three distinct eigenvectors in vector form:

$$\bar{x}_m = \begin{pmatrix} \dfrac{(\beta_{12} + \beta_{22} - \lambda_m)(\beta_{33} - \lambda_m)}{\beta_{32}(\beta_{11} + \beta_{21} - \lambda_m) - \beta_{31}(\beta_{12} + \beta_{22} - \lambda_m)} \\ \dfrac{\beta_{31}(\beta_{13} + \beta_{23}) - (\beta_{33} - \lambda_m)(\beta_{11} + \beta_{21} - \lambda_m)}{\beta_{32}(\beta_{11} + \beta_{21} - \lambda_m) - \beta_{31}(\beta_{12} + \beta_{22} - \lambda_m)} \\ 1 \end{pmatrix} \tag{26}$$

The transformation matrix, B, on the basis of previous eigenvectors can be written:

$$B = \left(\bar{x}_1\ \bar{x}_2\ \bar{x}_3\right) \tag{27}$$

This transformation matrix linearly relates the actual and transformed variables through the relation:

$$\bar{c}(s,x) = B\bar{b}(s,x) \tag{28}$$

where $\bar{c} = (\bar{c}_1\ \bar{c}_2\ \bar{c}_3)^T$ and $\bar{b} = (\bar{b}_1,\ \bar{b}_2,\ \bar{b}_3)^T$. Implementing the defined transformation on eq. (17) yields:

$$\frac{1}{\mathrm{Pe}_m}\frac{\partial^2 \bar{b}_m}{\partial x^2} - \frac{\partial \bar{b}_m}{\partial x} - s\lambda_m \bar{b}_m = -\lambda_m \bar{b}_{m,\mathrm{init}} \quad \text{where } \bar{b}_{m,\mathrm{init}} = \frac{\left(1 - \mathrm{e}^{-s\tau_{\mathrm{inj}}}\right)}{s|B|}\sum_{j=1}^{3} Z_{mj}\bar{c}_{j,\mathrm{init}},\ m = 1,2,3 \tag{29}$$

where Z is the adjoint of the transformation matrix B. Equation (29) represents a decoupled system of three advection-dispersion ODE. One can get the following explicit solutions by solving these equations independently:

$$\bar{b}_m(s,x) = \bar{b}_m(s,0)\mathrm{e}^{n_m x} + \frac{\bar{b}_{m,\mathrm{init}}}{s}\left(1-\mathrm{e}^{n_m x}\right) \text{ where } n_m = \frac{\mathrm{Pe}_m - \sqrt{\mathrm{Pe}_m^2 + 4s\lambda_i \mathrm{Pe}_m}}{2},\ m = 1,2,3 \quad (30)$$

The Laplace domain solutions are finally obtained by utilizing the initial, *c.f.* eq. (11) and boundary, *c.f.* eq. (12) conditions in the Laplace domain. These solutions are given:

$$\begin{aligned} c_m(s,x) = {} & \frac{(\beta_{12}+\beta_{22}-\lambda_m)(\beta_{33}-\lambda_m)-\beta_{32}(\beta_{13}+\beta_{23})}{\beta_{32}(\beta_{11}+\beta_{21}-\lambda_m)-\beta_{31}(\beta_{12}+\beta_{22}-\lambda_m)} b_1(s,x) + \\ & + \frac{\beta_{31}(\beta_{13}+\beta_{23})-(\beta_{33}-\lambda_m)(\beta_{11}+\beta_{21}-\lambda_m)}{\beta_{32}(\beta_{11}+\beta_{21}-\lambda_m)-\beta_{31}(\beta_{12}+\beta_{22}-\lambda_m)} b_2(s,x) + b_3(s,x) \end{aligned} \quad (31)$$

for m = 1, 2, 3. The analytical Laplace inversion is impractical in this case. However, the numerical Laplace inversion is applicable by approximating the integral of the inverse Laplace transformation through Fourier series [26].

Numerical case studies

In this section, some test problems are conducted to analyze the elution profiles of concentration and temperature obtained through the derived analytical solutions. A semi-discrete HR-FVS is also applied to numerically approximate the non-linear convection-diffusion PDE of the considered model, *c.f.* eqs. (1)-(5). The elution profiles generated through the analytical and numerical solutions are compared with each other. The MATLAB software is used to perform all computations. All the reference model parameters used in the test problems are selected from the typical ranges encountered in HPLC applications. The parameters of the test problem are similar to those given in [13, 15]. These parameters are summarized in tab. 1.

Table 1. Reference parameters used in the case studies

Parameters	Values
Length of column	L = 10 cm
Porosity	ϵ = 0.4
Interstitial velocity	u = 1.0 cm per minute
Dispersion coefficient	D_L = 0.02 cm^2 per minute
Heat capacity of solid times density	$c_p^S \rho^S$ = 40 kJ/ℓK
Heat capacity of liquid times density	$c_P^L \rho^L$ = 4 kJ/ℓK
Heat conductivity coefficient	λ_z = 0.08 kJ/cm per minute
Heat transfer coefficient	h_p = 1 W/cm^{2}K
Mass transfer coefficient	$k_1 = k_2$ = 100 mol per minute
Henry's constants	$a_{1,\mathrm{ref}}$ = 1.4, $a_{2,\mathrm{ref}}$ = 2.0
Enthalpy of adsorption	ΔH_A = −2 kJ/mol
Initial concentrations	$c_{i,\mathrm{init}}$ = 0 mol/ℓ (i = 1, 2)
Inlet concentrations	$c_{i,\mathrm{in}}$j = 1 mol/ℓ (i = 1, 2)
Initial temperature	T_{init} = 300 K
Inlet temperature	T_{inj} = 300 K
Reference temperature	T^{ref} = 300 K
Injection time	t_{inj} = 5 minutes

Effect of enthalpy of adsorption $\Delta H_{A,i}$ (i = 1,2)

Figure 1 compares the results of analytical solutions for isothermal case ($\Delta H_{A,i} = 0$ kJ/mol) in plots (a) and (b) and for non-isothermal cases ($\Delta H_{A,i} \neq 0$ kJ/mol) in plots (c) and (d). Here, two different values of mass transfer coefficients, k_i (i = 1,2), are taken into account along with the assumptions that $k_1 = k_2$ and $\Delta H_{A,1} = \Delta H_{A,2}$. Moreover, the initial and inlet temperatures were set equal to the reference temperature, *i.e.* $T_{\text{init}} = T_{\text{inj}} = T^{\text{ref}}$. It is evident from plots (a) and (b) that isothermal operating condition leads to steady-state temperature profile. On the other hand, the non-isothermal operating condition significantly produces fluctuations in the temperature profile. Further, the concentration and the temperature profiles are sharper and have narrower peaks for larger values of mass transfer coefficients, k_i = 100 mol per minute (i = 1, 2), and are broadened for smaller values of mass transfer coefficients, k_i = 1 mol per minute (i = 1, 2), which is an indication of slow chromatographic process. Moreover, it can be observed that adsorption enthalpy has remarkable effect on temperature profile but it does not affects the concentration profile of both components.

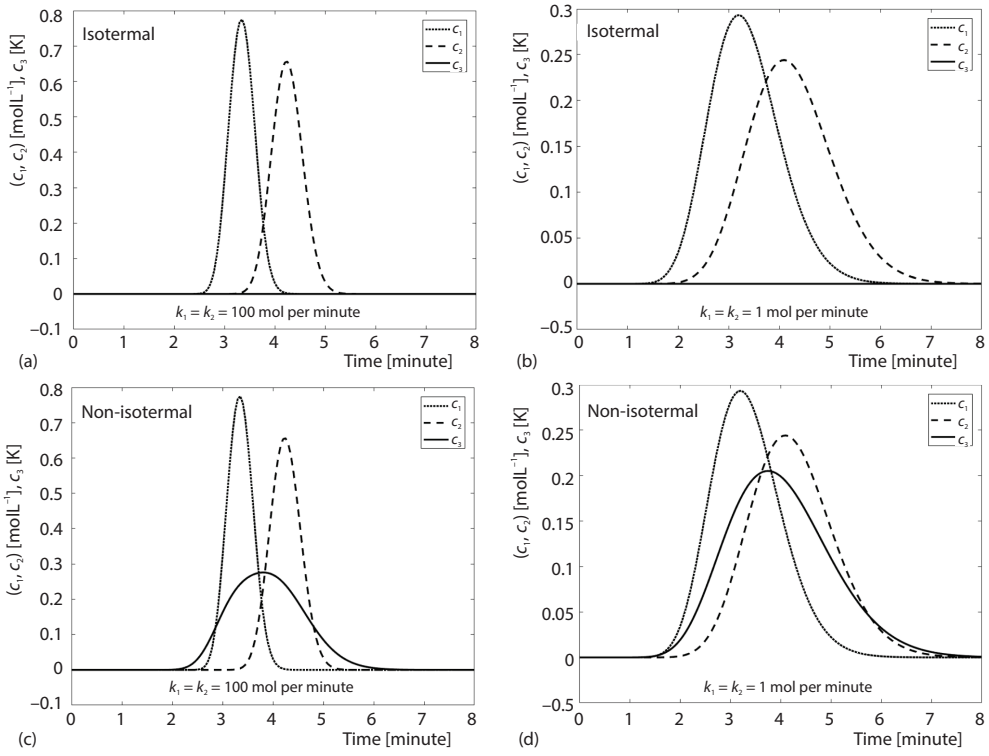

Figure 1. Effects of mass transfer coefficients (k_i, i = 1, 2) on concentrations and temperature profiles under isothermal condition, $\Delta H_A = 0$ (a) and (b) and under non-isothermal condition, $\Delta H_A \neq 0$, (c) and (d); all other parameters are given in tab. 1

Comparison of analytical and numerical solutions ($\Delta H_{A,i} \neq 0$)

A comparison of analytical solutions for linearized isotherm, *c.f.* eq. (31), with the numerical solutions of HR-FVS, *c.f.* eq. (5), for different values of ΔH_A, which is assumed to be identical for both components, is shown in figs. 2-4. It is evident from the figures that the

numerical solution accurately converges to analytical solution when the magnitude of enthalpy of adsorption is taken to be small, *i.e.* $\Delta H_A = -2, -10$ kJ/mol. Where as, for larger magnitude of enthalpy of adsorption, *i.e.* $\Delta H_A = -40$ kj/mol, the analytical solutions for linearized isotherm and numerical solutions for non-linear isotherm start deviating from each other which justify the linearization of the adsorption isotherm. Once again, the analysis is done for two different values of mass transfer coefficients.

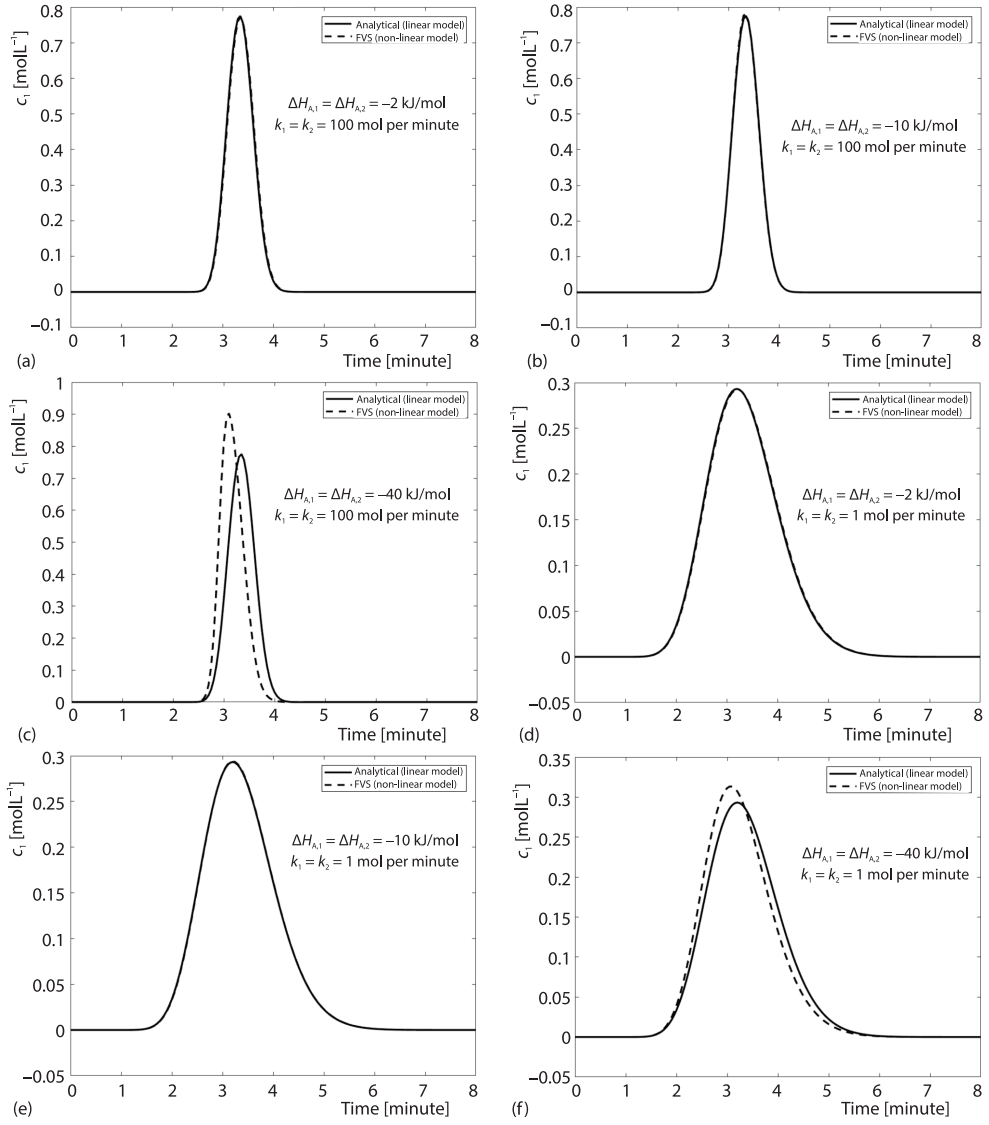

Figure 2. A comparison of concentration profiles of the first component obtained from analytical and numerical solutions for two different values of mass transfer coefficient $k_i = 1$ or 100 mol per minute ($i = 1, 2$). when $\Delta H_{A,i} \neq 0$

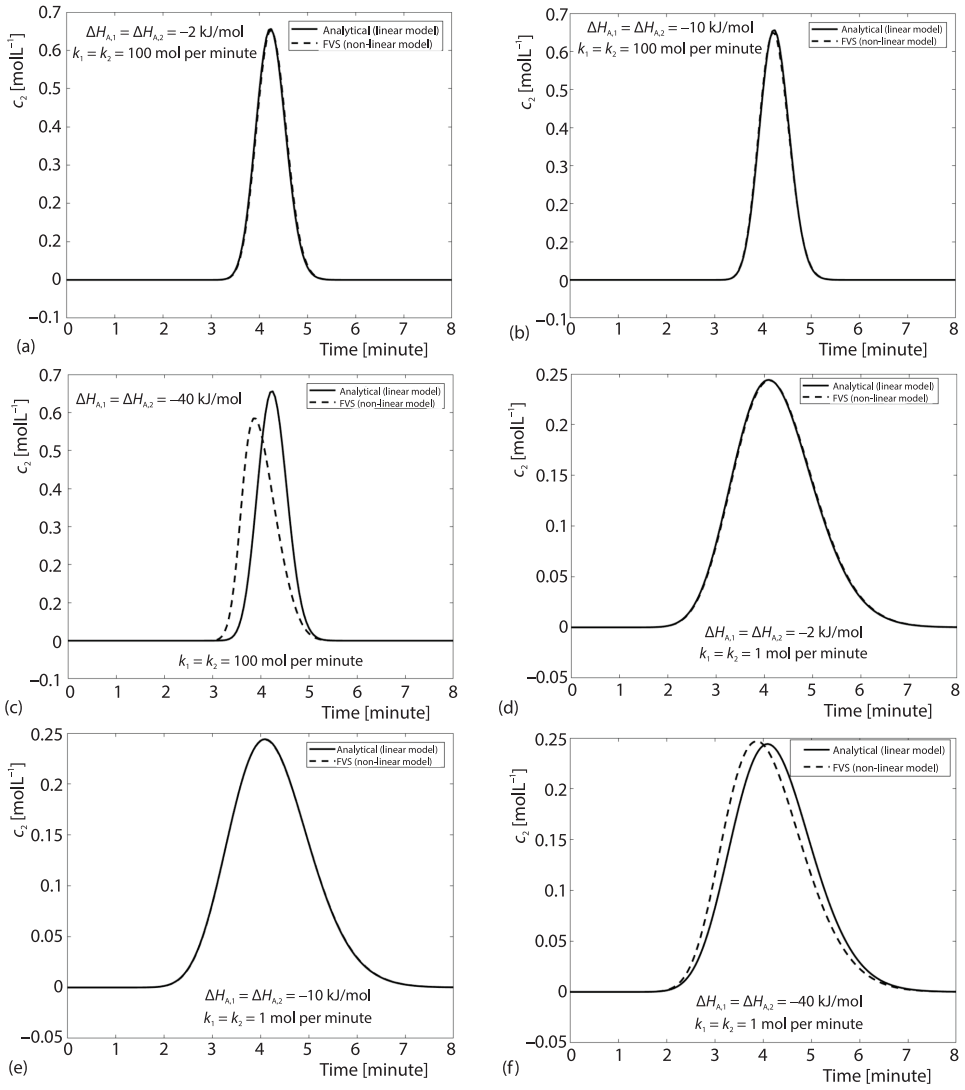

Figure 3. A comparison of concentration profiles of the second component obtained from analytical and numerical solutions for two different values of mass transfer coefficient $k_i = 1$ or 100 mol per minute ($i = 1, 2$) when $\Delta H_{A,i} \neq 0$

Effect of the ratio C_e/C_f

Figure 5 depicts the effect of the ratio of specific heat C_e/C_f on concentrations and temperature profiles. For the case when $C_e/C_f < 1$, the adsorption peak of the temperature is moving fast while the desorption peak of temperature is moving slower and is coupled with the concentration profiles. This indicates that the concentration profiles and the desorption peak of temperature are moving with the same speed, *c.f.* plots (a) and (d). Hence, during the passage of the mobile phase through the stationary phase, adsorption is taking place quickly and releasing less amount of energy while desorption takes longer time to complete. Also, the extent of

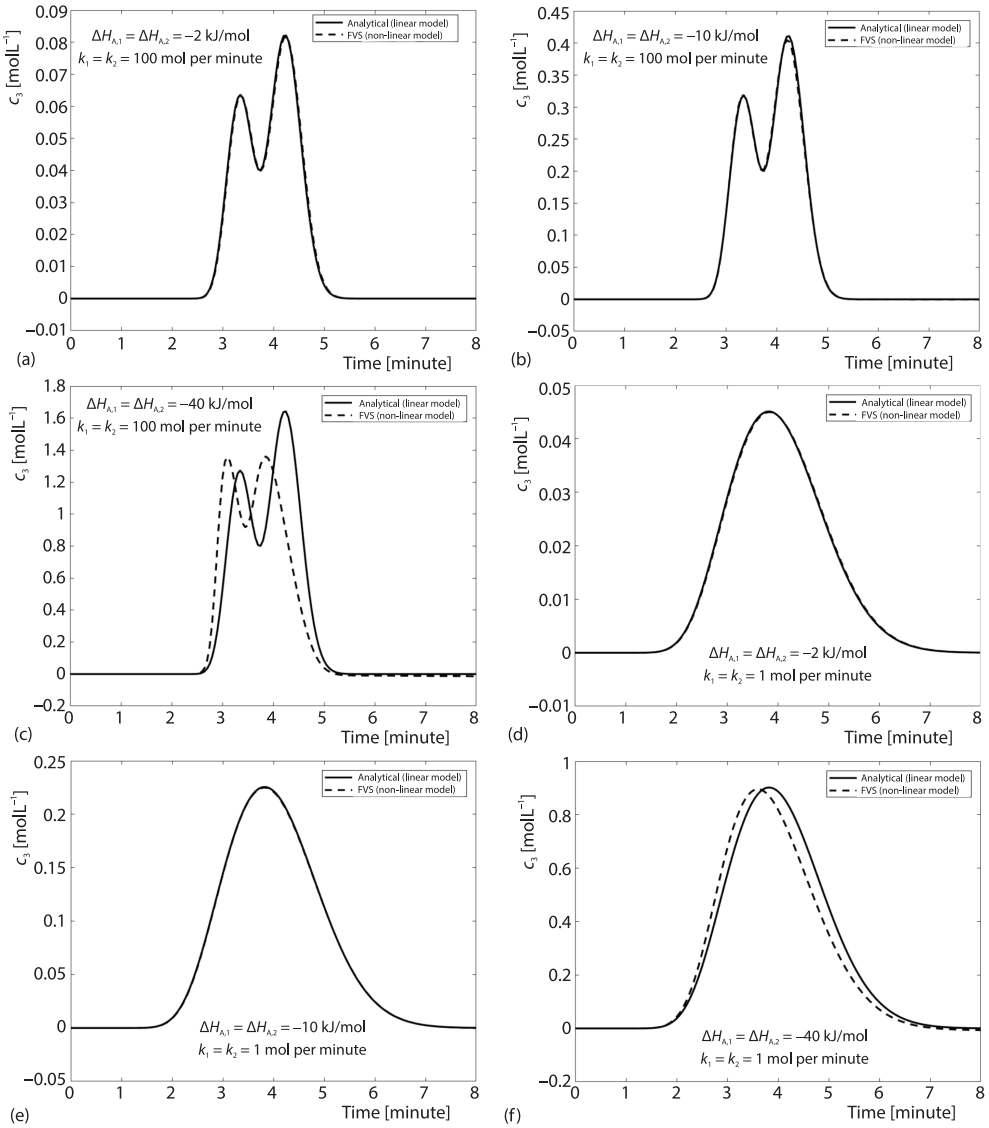

Figure 4. A comparison of temperature profiles obtained from analytical and numerical solutions for two different values of mass transfer coefficient $k_i = 1$ or 100 mol per minute ($i = 1, 2$) when $\Delta H_{A,i} \neq 0$

adsorption is high and as soon as the desorption starts, the concentration profiles start emerging at the column outlet. For the case when $C_e/C_f = 1$, it can be seen from the plots (b) and (e) that both the concentration and temperature profiles are moving at almost the same speed and, thus, releasing a high amount of energy during adsorption. When $C_e/C_f > 1$, the adsorption peak of temperature is coupled with the concentration profiles, see plots (c) and (f). It can also be observed that the elution profiles are narrower and more concentrated for $k_i = 100$ ($i = 1, 2$) and are less concentrated and broadened for $k_i = 1$($i = 1, 2$).

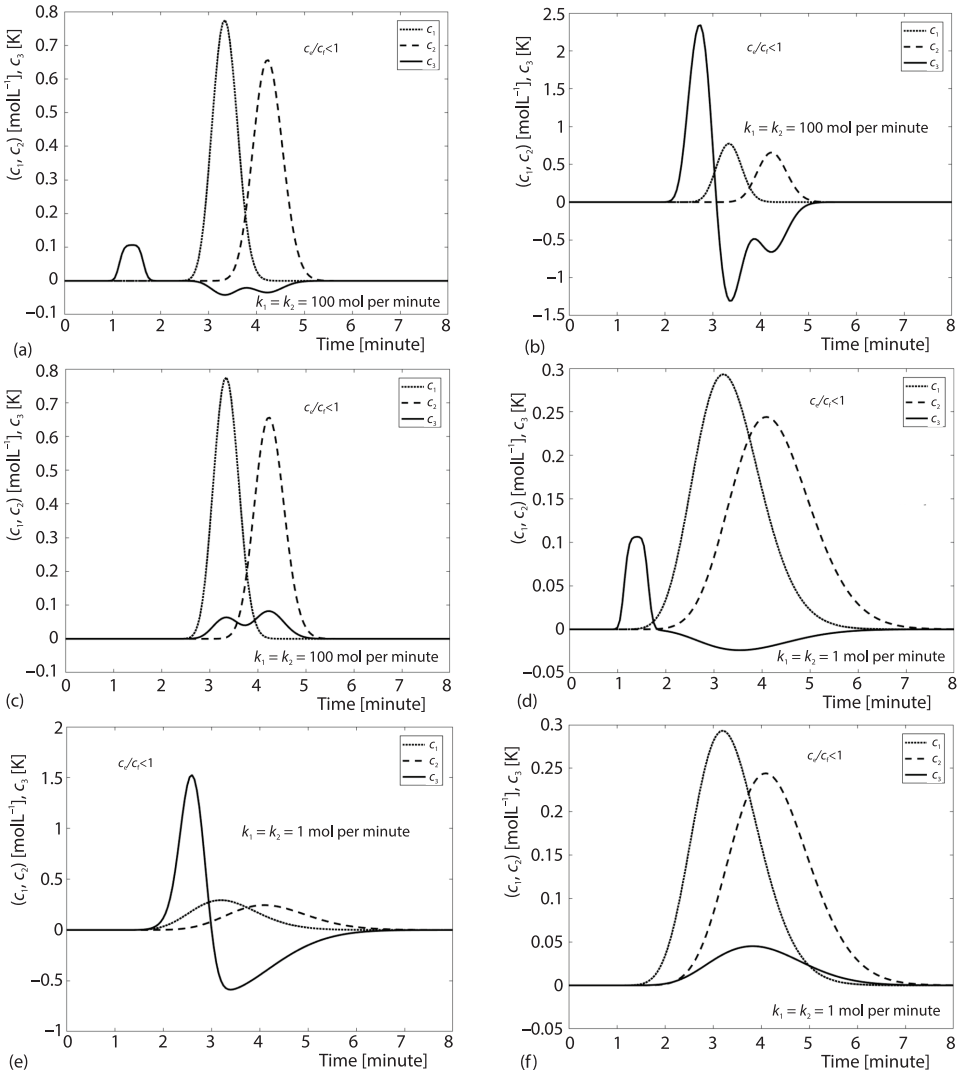

Figure 5. The effect of ratio C_e/C_f on temperature and concentrations profiles for k_i (i = 1, 2) = 1 or 100 mol per minute

Effect of the temperature of the injected sample

Figure 6 demonstrates the effect of variation in the temperature of the injected sample. It can be easily observed from plots (a) and (c) that an increase in the temperature of the injected sample (hot injection, $T_{inj} < T^{ref}$) enlarges the fast-moving adsorption peak of the temperature to its maximum value, while reducing the height of the desorption peak. Which means that during the adhesion of the injected mixture within the stationary phase, adsorption takes place quickly and, thus, releases an extra amount of energy. This release in energy will be greater for larger values of the injected sample temperature. In the case of cold injection ($T_{inj} < T^{ref}$), contrary to the previous case, it can be easily seen from plots (b) and (d) that desorption peak of the temperature profile is gradually increasing in the negative direction. The endothermal desorption

peak diminishes in this case. Further, both cases have depicted no visible effects on the concentration profiles due to the considered linearization.

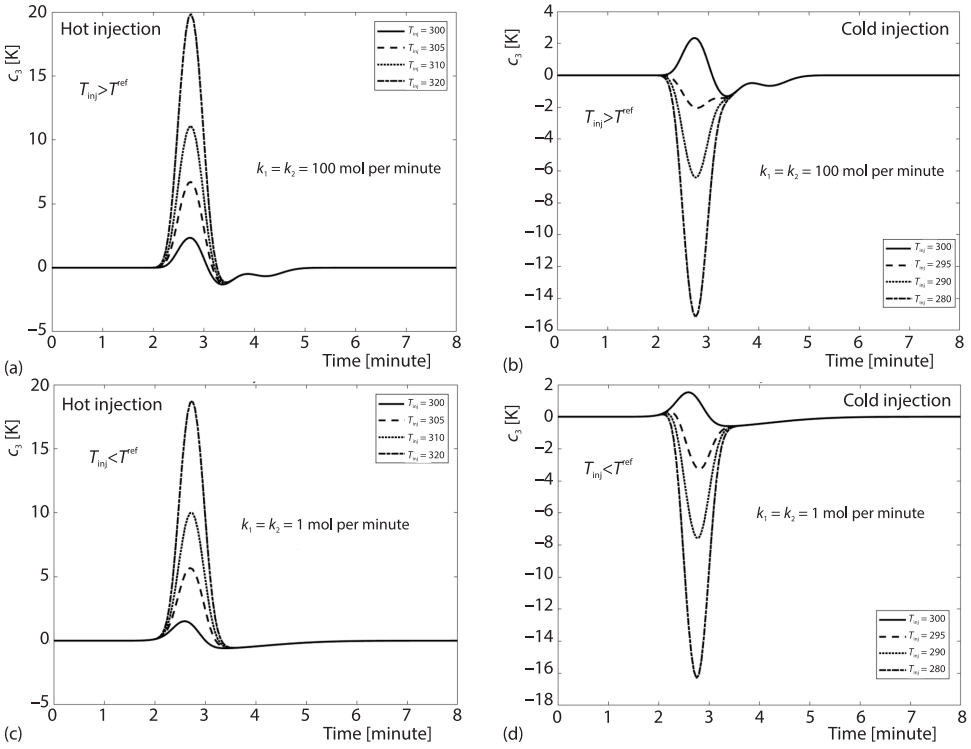

Figure 6. The effect of $T_{inj} \neq T^{ref}$ on profiles for $C_e/C_f = 1$; here, two different values of mass transfer coefficients are considered; all other parameters are given in tab. 1

Conclusion

A two-component linearized non-isothermal and non-equilibrium LKM of liquid chromatography was formulated and solved analytically to study the thermal effects on the under-lying separation process inside the chromatographic column. General analytical solutions were derived for linearized isotherm through successive implementation of the Laplace transformation, Tschirnhaus-Vieta approach, the decoupling technique of linear transformation and the conventional solution method of ODE. To get required solutions in the actual time domain, numerical Laplace inversion method was used, because analytical inversion of the Laplace transformation was not applicable. In addition, to gain further confidence on the obtained analytical solutions, the full non-linear model equations, incorporating non-linear isotherms, were also approximated numerically by a high resolution finite volume method. Several case studies were carried out to determine applicability ranges of our linearized solutions. The derived and carefully validated solutions are found well applicable for small value of enthalpy of adsorption. These results indicate that developed analytical and numerical methods are accurate. These results can be utilized in further systematic studies of non-isothermal chromatographic processes to optimize factors like purity, productivity, eluent consumption and production rate.

Nomenclature

a_j^{ref} – j^{th} component reference Henry's constant, [–]
$c_{i,init}$ – initial concentrations, [molℓ^{-1}]
$c_{i,inj}$ – inlet concentration, [molℓ^{-1}]
c_j – mobile phase concentration, [molℓ^{-1}]
$c_P^L\rho^L$ – heat capacity of liquid times density, [kJℓ^{-1}K^{-1}]
$c_P^S\rho^S$ – heat capacity of solid times density, [kJℓ^{-1}K^{-1}]
D_L – axial dispersion coefficient, [cm^{2}min^{-1}]
ϵ – total porosity, [–]
F – phase ratio, [–]
ΔH_A – enthalpy of adsorption, [kJmol^{-1}]
h_p – heat transfer coefficient, [Wcm^{-2}]
k – mass transfer coefficient, [molmin^{-1}]
L – length of the column, [cm]
q_j – solid phase concentration,[molℓ^{-1}]
T – mobile phase temperature, [K]
T_{init} – initial temperature, [K]
T_{inj} – inlet temperature, [K]
T_S – stationary phase temperature, [K]
T^{ref} – reference temperature, [K]
t – time co-ordinate, [min]
t_{inj} – injection time, [min]
u – linear velocity, [cmmin^{-1}]
z – axial co-ordinate, [–]

Greek symbol

λ_L – heat conductivity coefficient, [kJcm^{-1}min^{-1}]

References

[1] Guiochon, G., Preparative Liquid Chromatography, *Journal Chromatogr. A* ., *965* (2002), 1-2, pp. 129-161
[2] Guiochon, G., Lin, B., *Modelling for Preparative Chromatography*, Academic Press., Amsterdam, The Netherlend, 2003
[3] Dunlap, C. J., *et al*., Zirconia Stationary Phases for Extreme Separations, *Anal. Chem*., *73* (2001), 21, pp. 598A-607A
[4] Yang, Y., Subcritical Water Chromatography: A Green Approach to High-Temperature Liquid Chromatography, *Anal. Chem*., *30* (2007), 8, pp. 1131-1140
[5] Greibrokk, T., Andersen, T., High Temperature Liquid Chromatography, *Journal Chromatogr. A*., *1000* (2003), 1-2, pp. 743-755
[6] Smith, R. M., Burgess, R. J., Superheated Water as an Eluent for Reversed-Phase High-Performance Liquid Chromatography, *Journal Chromatogr. A*., *785* (1997), 1-2, pp. 49-55
[7] Teutenberg, T., *et al.*, Separation of Selected Anticancer Drugs Using Superheated Water as the Mobile Phase, *Anal. Chem*., *73* (2001), 16, pp. 3896-3899
[8] Genowefa, H., Jerzy, S., K., The Effect of Temperature on the Efficiency Parameters in Adsorptive Liquid Chromatography, *JHRC*, *4* (1981), 1, pp. 27-32
[9] Cerro, R. L., Smith, J. M., Effects of Heat Release and Non-Linear Equilibrium on Transient Adsorption, *Ind. Eng. Chem. Fundam*., *8* (1969), 4, pp. 796-802
[10] Hayat, A., *et al*., Theoretical Analysis of Forced Segmented Temperature Gradients in Liquid Chromatography, *Processes*, *7* (2019), 11, pp. 846-864
[11] Brandt, A., *et al*., Temperature Gradients in Preparative High-Performance Liquid Chromatography Columns, *Journal Chromatogr. A*., *769* (1997), 1, pp. 109-117
[12] McCalley, D. V., Effect of Temperature and Flow-Rate on Analysis of Basic Compounds in High-Performance Liquid Chromatography Using a Reversed-Phase Column, *Journal Chromatogr. A*, *902* (2000), 2, pp. 311-321
[13] Sainio, T., *et al*., Thermal Effects in Reactive Liquid Chromatography, *Chem. Eng. Sci*., *62* (2007), 18-20, pp. 5674-5681
[14] Sainio, T., Zhang, L., Seidel-Morgenstern, A., Adiabatic Operation of Chromatographic Fixed-Bed Reactors, *Chem. Eng. J*., *168* (2011), 2, pp. 861-871
[15] Vu, T. D., Seidel-Morgenstern, A., Quantifying Temperature and Flow Rate Effects on the Performance of a Fixedbed Chromato-Graphic Reactor, *Journal Chromatogr. A*., *1218* (2011), 44, pp. 8097-8109
[16] Javeed, S., *et al*., Parametric Study of Thermal Effects in Reactive Liquid Chromatography, *Chem. Eng. J*., *191* (2012), May, pp. 426-440
[17] Qamar, S., *et al*., Theoretical Analysis of the Influence of Forced and Inherent Temperature Fluctuations in an Adiabatic Chromatographic Column, *Chem. Eng. Sci.*, *161* (2017), Apr., pp. 249-264
[18] Qamar, S., *et al*., Theoretical Investigation of Thermal Effects in Non-Isothermal Non-Equilibrium Reactive Liquid Chromatography, *Chem. Eng. Res. Design*., *115* (2016), Part A, pp. 145-159
[19] Qamar, S., Theoretical Investigation of Thermal Effects in an Adiabatic Chromatographic Column Using a Lumped Kinetic Model Incorporating Heat Transfer Resistances, *Ind. and Eng. Chem. Res*., *57* (2018), 6, pp. 2287-2297

[20] Garver, R., The Tschirnhaus Transformation. Annals of Mathematics, *JSTOR*., *29* (1927), 1/4, pp. 319-333
[21] Rice, R. G., Do, D. D., *Applied Mathematics and Modelling for Chemical Engineers*, Wiley-Interscience, New York, USA, 1995
[22] Javeed, S., Analysis and Numerical Investigation of Two Dynamic Models for Liquid Chromatography, *Chem. Eng. Sci*., *90* (2013), Mar., pp. 17-31
[23] Guiochon, G., *Fundamentals of Preparative and Non-Linear Chromatography*, 2nd ed., Elsevier Academic Press, New York, USA, 2006
[24] Sajonz, P., *et al*., Application of the Shock Layer Theory to the Determination of the Mass Transfer Rate Coefficient and its Concentration Dependence for Proteins on Anion Exchange Columns, *Biotechnol. Prog*., *13* (2008), 2, pp. 170-178
[25] Rehman, J. U., *et al*., Study of Thermal Effects in Twocomponent Non-Isothermal Liquid Chromatography Considering Thermally Insulated Columns, *Ind. Eng. Chem. Research*., *57* (2018), 44, pp. 15084-15095
[26] Durbin, F., Numerical Inversion of Laplace Transforms: An Efficient Improvement to Dubner and Abate's Method, *Comput. J*., *17* (1974), 4, pp. 371-376

Paper submitted: February 27, 2020
Paper revised: May 5, 2020
Paper accepted: May 8, 2020